JOURNAL OF GEOPHYSICAL RESEARCH, VOL. 98, NO. B7, PAGES 11,953–11,966, JULY 10, 1993

On the Role of the Upper Plate in Great Subduction Zone Earthquakes

ROBERT MCCAFFREY

Department of Earth and Environmental Sciences, Rensselaer Polytechnic Institute, Troy New York

At subduction zones where convergence is not perpendicular to the trench (i.e., oblique), slip vectors of interplate thrust earthquakes are often systematically deflected away from the expected plate vector, probably by deformation of the leading edge of the upper plate. Near the epicenters of great thrust earthquakes of $M_w \geq 8.0$ in this century that occurred at trenches, systematic deflections of slip vectors for recent (1977-1992.5) interplate thrust earthquakes are significantly less than global averages. Statistical tests show that great earthquakes nucleate where deviations of slip vectors (residuals) are smaller and plate convergence is faster but not preferentially where the angle of obliquity is smaller than global averages. The small slip vector residuals suggest that great earthquakes nucleate where forces in the forearc due to plate convergence are sustained elastically, rather than anelastically, and that shear stress on subduction thrust faults with great earthquakes is not necessarily higher than on faults without them. Shear stress magnitude is less important than rheology in determining the seismic behavior of subduction zones. An observed decrease in the slip vector residuals with increasing rates of trench-normal convergence is interpreted as evidence that the forearc is increasingly cooled and strengthened by faster subduction. For the forearc to cool with increasing convergence rate, the shear stress on the subduction thrust fault must be less than about 40 MPa. Lower temperatures on the fault surface and the possibility that thrust faults below undeforming forearcs are smoother than those below deforming forearcs both act to increase the frictional instability of the fault zone. Great thrust earthquakes at subduction zones seem to occur where convergence is fast and the forearc is cool and predominantly elastic. The ability of the forearc of the upper plate to store elastic strain energy appears to be a major factor controlling where great subduction thrust earthquakes can and cannot occur.

INTRODUCTION

Understanding the factors that control where great subduction zone earthquakes occur is an important quest of seismology. Relationships have been made between great earthquake distribution and convergence rate, plate age, dip angle, absolute motions of the plates, trench sediments, seamounts, etc. [*Kelleher et al.*, 1974; *Kelleher and McCann*, 1976; *Uyeda and Kanamori*, 1979; *Ruff and Kanamori*, 1980; *Peterson and Seno*, 1984; *Jarrard*, 1986; *Ruff*, 1989; *Cloos*, 1992] although some of these correlations are now disputed [*Pacheco et al.*, 1993]. Proposed correlations between earthquake size or moment release rate, plate age and convergence rate have led to the conclusion that normal stress on the thrust fault is most important in the distribution of great earthquakes [*Ruff and Kanamori*, 1980; *Peterson and Seno*, 1984]. However, the conditions that allow great earthquakes to occur must include the ability of the upper plate to build and maintain shear strain elastically during the period of time between the great earthquakes. I describe a method to characterize the rheologies of the forearcs of subduction zones and then show a strong correlation between the occurrence of great subduction zone thrust earthquakes and forearcs that appear to behave elastically in response to the stress acting across the thrust fault between the plates. I argue that it is the rheology of the forearc more than the shear stress magnitude that determines where great earthquakes occur.

Because oblique convergence, defined as convergence that is not perpendicular to the trend of the trench (Figure 1), produces a shear stress on the upper plate parallel to the trench, the response of a forearc to shear stress can be estimated by examining evidence for deformation in regions of oblique subduction. Tectonically significant arc-parallel deformation rates in the forearc are evident in deflections of subduction earthquake slip vectors away from the plate convergence vector; we call this deviation the slip vector residual. If slip vector residuals are small when the angle of obliquity is large then the forearc can be said to respond elastically (i.e., no time dependent anelastic strain in the forearc) to the arc-parallel shear force produced by oblique convergence. If the upper plate cannot support such shear stress by elastic strain alone, it will undergo permanent deformation under oblique convergence and the slip vector residuals will be large. The approach used here is to examine the epicentral regions of great subduction zone thrust earthquakes to determine if slip vectors from recent earthquakes are parallel to the plate vector or deviate significantly from it. I take a different approach from that of *Jarrard* [1986], who used geologic evidence for arc-parallel strike-slip faulting to infer deformation rates of forearcs. However, reliable geologic constraints on modern slip rates for arc-parallel faults are few. Deflections of slip vectors may provide a better indication of the overall deformation rate in the forearc, although this approach may have its own pitfalls, particularly in the brevity of the sampling period.

SLIP VECTOR RESIDUALS AND CONVERGENCE OBLIQUITY

Slip vector residuals are the differences between the observed slip vectors from thrust earthquakes at subduction zones and the plate convergence directions predicted by rigid plate rotation poles (Figure 1). Slip vectors of earthquakes that are due to thrusting of oceanic lithosphere beneath the forearcs of the island arcs are derived largely from the Harvard centroid-moment tensor (CMT) solutions for the time 1977 through June 1992 [e.g., *Dziewonski et al.*, 1983]. Earthquakes from

Paper number 93JB00445.
0148-0227/93/93JB-00445$05.00

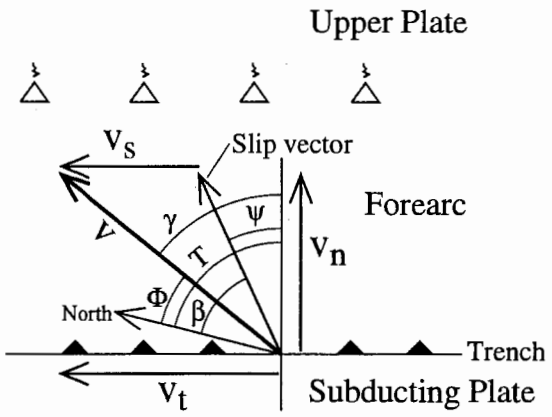

v = predicted plate convergence vector

T = trench-normal azimuth

Φ = plate motion azimuth

β = slip vector azimuth

ψ = trench normal - slip vector = T - β

Obliquity: $\gamma = T - \Phi$

Slip vector residual: $\Delta\beta = \beta - \Phi$

Forearc slip rate:

$v_s = v (\sin\gamma - \cos\gamma \tan\psi)$

Fig. 1. Geometry of oblique convergence. The reference frame is the upper plate beyond the volcanic arc. The velocity vector V (at azimuth ϕ) shows the motion of the subducting plate relative to the upper plate and makes an angle γ (the obliquity) with respect to the trench-normal azimuth (T). If the forearc deforms so that it moves at a rate V_s relative to the upper plate then the slip vector azimuth β is rotated toward the trench-normal azimuth by an amount which is called the slip vector residual; $\Delta\beta = \beta - \phi$. If the forearc deforms elastically so that $V_s 0$ then $\beta = \phi$ and the slip vector residual is zero. Note that because β, ϕ, and T are azimuths, the slip vector residual and obliquity can be positive or negative. Vn and Vt are the trench-normal and trench-parallel components of the plate vector V.

which the slip vectors are taken meet the following criteria: the focal depth is less than 60 km, the rake angle is between 0° and 180° (i.e., a thrust component to the mechanism), the strike of the nodal plane is within 90° of the local strike of the trench, the dip of the fault plane is less than 40° and is in the same direction as the subduction thrust fault, and of course the earthquake occurred landward of a trench. These criteria are intended to include only earthquakes that occur on the plate interface. The large deviation between the trench and fault plane strikes is allowed because the strike of a plane dipping at only a few degrees is very poorly determined by seismological methods; however, orientation of the slip vector, the normal to the auxiliary plane, is typically quite well determined for these events. These slip vectors were supplemented by those compiled by *Ranken et al.* [1984] for the Nankai trough (where there are no CMT solutions), non-CMT slip vectors used in NUVEL-1 [*DeMets et al.*, 1990], and additional non-CMT slip vectors from the Aleutian, Kurile, Mid America, and South American trenches provided by C. DeMets and D. Argus.

To estimate the obliquity at each point along the trenches, I first estimate the trench outlines by finding the deepest points in the seafloor using the database DBDB5 which comprises 5 min (approximately 8 km) averages of bathymetry. These points are smoothed by calculating values every 0.1° (approximately 11 km) with a least squares spline using a correlation distance of 2° of arc (220 km). The trench-normal is the azimuth perpendicular to the trench trend, points toward the hanging wall side, and is calculated with respect to this smoothed, discretized curve. Expected convergence directions are calculated from the relative rotation poles of *DeMets et al.* [1990] for most trenches, from the poles of *Seno et al.* [1987] for trenches bordering the Philippine Sea plate, and from *McCaffrey* [1991] for the Java trench.

Trenches included in this analysis are the Aleutian, Kuriles, Japan, Nankai, Ryukyu, Izu, Mariana, Java, Solomon, New Hebrides, Tonga, Sandwich, Antilles, South America and Middle America (Figure 2). For most of these, the plate convergence direction is known with a few degrees uncertainty independently of subduction zone slip vectors [*DeMets*, 1993]. Others, such as the Java, Mariana, and Antilles arcs, where the pole of rotation is poorly known, must have sections of large obliquity owing to their great curvature. Nevertheless, I test the effect of ignorance of the expected convergence direction for several trenches by using a pole of rotation that minimizes the slip vector residuals along them.

The Ryukyu trench probably has nearly normal convergence along most of its length [*Seno et al.*, 1987] but the uncertainty in the convergence direction is not critical to my arguments because no great earthquakes have occurred there. At the Nankai trough, where there are great earthquakes, the convergence direction is not known independently of the slip vectors. Since the slip vectors are quite oblique to the trench [*Ranken et al.*, 1984], if forearc deformation does occur it does not significantly decouple the normal and shear components of the motion; i.e., the forearc has a strong elastic component. The significance of the Median Tectonic line northwest of the Nankai trough is not clear as the slip rate (which is probably less than 10 mm/yr) and even the sense of slip are debated [see *Ranken et al.*, 1984]. The Philippine trench is excluded because the plate convergence direction is exceptionally poorly known there. The Philippines are not rigidly connected to Eurasia so the Philippine Sea - Eurasia pole of rotation is not appropriate for the Philippine trench. The New Britain trench is also excluded due to ignorance of the expected convergence direction there.

Slip vectors, plate vectors, and trench normals are collected in forearc bins (Figure 2), ranging from 75 to 200 km wide, along each trench (bin limits are determined independently of the locations of the great earthquakes). In each bin I calculate the average slip vector residual (the mean of the differences between the slip vector azimuths and the expected plate convergence azimuth at the epicenters of the earthquakes) and the obliquity (mean trench-normal azimuth minus the mean plate convergence azimuth) and their standard errors. While the form of the statistical distribution of the individual slip vector residuals is not known, the means of the residuals and obliquities in bins should have a normal distribution according to the central limit theorem. Binning also decreases the bias that might arise because some trenches have more slip vectors than others. Most of the statistical tests are done on the mean values from the bins, although the distributions of the individual slip vector residuals are also examined. In calculating the means and standard deviations of the slip vectors in bins, each slip vector is given equal weight; other

weighting schemes (shown below) make little difference in the means and standard errors [*DeMets*, 1992; *McCaffrey*, 1993] and have no bearing on the conclusions. The distribution of slip vector residuals and obliquities for the world's trenches are then compared for those bins in which great earthquakes have and have not occurred.

GREAT EARTHQUAKES

The main point of this work is that great subduction zone thrust earthquakes over the past 90 years occurred at sections of trenches where slip vector residuals are small and convergence rates are high but not where obliquity is small, compared to global trends. A great earthquake is one with a surface-wave magnitude M_s or moment magnitude M_w [*Kanamori*, 1986] greater than or equal to 8.0. Few earthquakes prior to 1940 have had M_w determined (Table 1) so for these I use *Abe's* [1981] M_s values. Because my main concern is whether or not an earthquake was greater than M_w=8, saturation of the M_s scale has little bearing on this analysis because the M_s and M_w scales are nearly equivalent at $M_s \approx 8$ and for $M_s > 8$, M_w is greater than M_s. In the Abe catalog there are 28 earthquakes of $M_s \geq 8$ that fall within the sections of the arcs examined here. I also include four earthquakes listed by *Ruff* [1989] and four listed by *Lay et al.* [1982] as having $M_w \geq 8.0$ even though they are assigned $M_s < 8.0$ by *Abe* [1981], and four recent earthquakes with seismic moments of greater than 10^{21}N m from the CMT solutions, for a total of 40 events (Table 1 and Figure 2). I also keep those earthquakes that have had their M_s downgraded to less than 8.0 by *Pacheco and Sykes* [1992].

Five of the great subduction earthquakes listed in Table 1 are excluded from the statistical analysis because the convergence obliquity near them is poorly constrained. These are the 1923 Japan earthquake because it occurred near the junction of the Nankai, Japan and Izu trenches, the 1939 Solomon Islands earthquake that occurred near the intersection of the Woodlark Rift with the Solomon trench, and a pair of earthquakes in 1971 at the northeastern corner of the New Britain trench (a triple junction). The 1964 Alaska earthquake is also excluded because it occurred at the eastern end of the Aleutian trench where the trench orientation is poorly constrained. Nevertheless, the slip vectors for recent earthquakes trenchward of it are within 10° of the expected plate vector [*Perez and Jacob*, 1980; *DeMets et al.*, 1990]. The addition of this event to the analysis would either strengthen the correlation between slip vectors and plate vectors near great earthquakes (if the obliquity there is large) or have no bearing on it (if the obliquity is small).

Listed in Table 1 for each great earthquake are the approximate obliquity and the average slip vector residual for events within 200 km of the great earthquake's epicenter. The

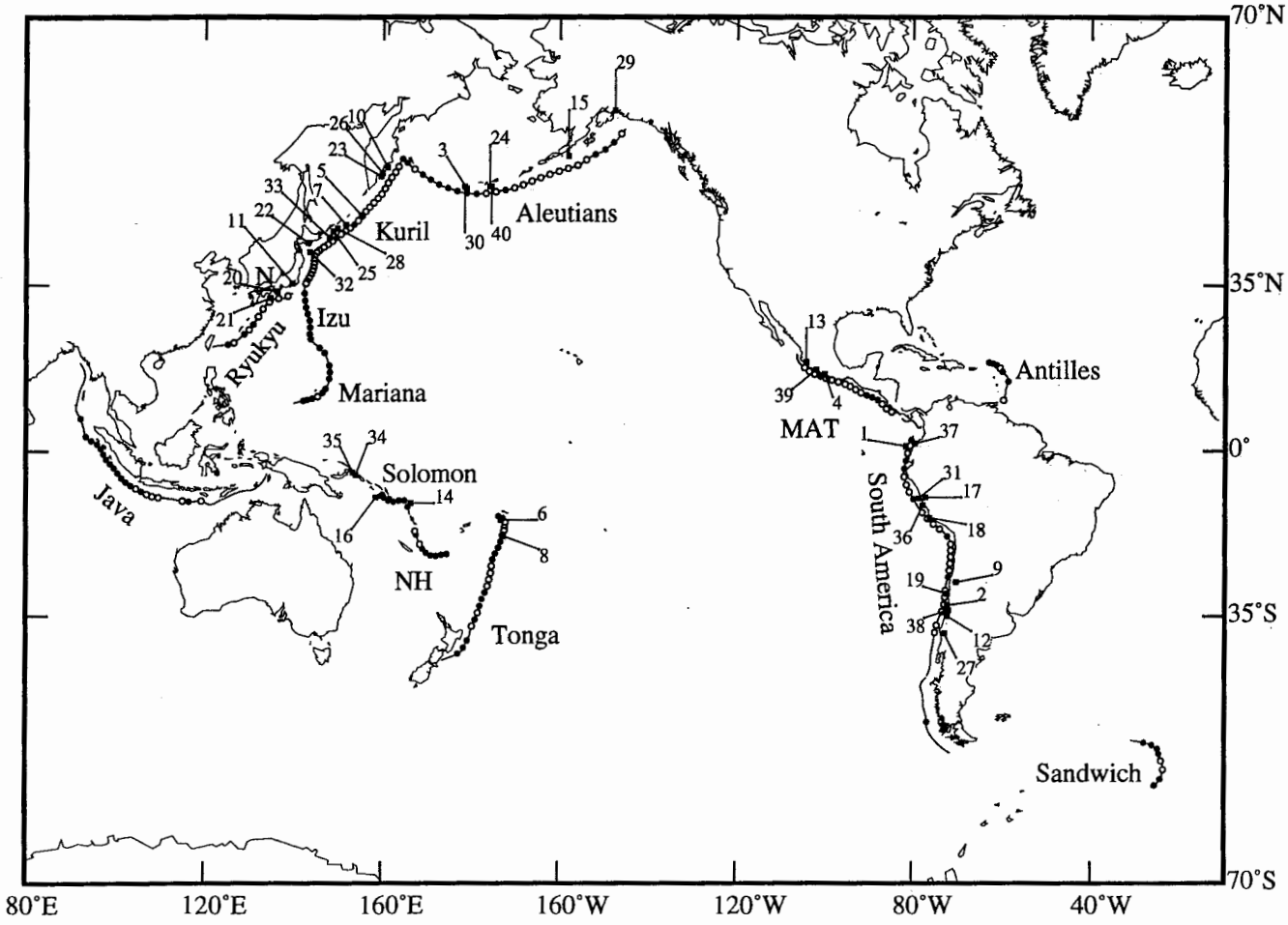

Fig. 2. Trenches included in the analysis are shown by lines; small circles indicate centers of forearc bins and are filled when the absolute value of the average slip vector residual for the bin is greater than 10°. Earthquakes of $M_w \geq 8.0$ are labeled by event number given in Table 1. NH, New Hebrides; N, Nankai; MAT, Middle America trench.

largest well-determined average slip vector residual near a great earthquake is 20.5° for event 30 (1965 Rat Islands earthquake) in the Aleutians where the obliquity is 50° (Table 1). The slip vector residuals appear to be small compared to the obliquity but in order to see if they are indeed smaller than normal we must compare them to the global distribution of slip vectors.

Earthquakes of $M_w \geq 8.0$ can rupture hundreds of kilometers along the trench so it may seem inappropriate to place them in bins less than 200 km wide. This can be rationalized in two ways. First, the reported hypocenters of the earthquakes are based on arrival times of P waves and thus represent the nucleation points of the earthquakes. Hence, the following arguments concern the nucleation points of great earthquakes. The second point is that although some of these earthquakes may rupture across several bins, the slip vector residuals vary smoothly from bin to bin along a trench and it makes little difference if the earthquake is assigned to a neighboring bin or if the bin width is increased [*McCaffrey*, 1993].

The 35 great earthquakes are contained in 31 forearc bins (for brevity bins in which $M_w \geq 8.0$ events occurred are called M8 bins). In general, again we see that earthquakes of $M_w \geq 8.0$ occur where slip vectors are nearly parallel to the expected plate convergence vector even though the obliquity can be as high as 60° (Table 2 and Figures 3 and 4). Only one M8 bin has a well-constrained absolute average slip vector residual larger than 20°; 22±11° in the central Aleutians where the obliquity is 50±3° (Table 2). Most slip vector residuals are less than 10°. The slip vector residuals for M8 bins appear to be independent of obliquity (Figure 4a) and with only 4 exceptions, great earthquakes appear to occur where convergence is faster than 60 mm/yr (Figure 4b) in accord with earlier suggestions [*Ruff and Kanamori*, 1980; *Peterson and Seno*, 1984].

STATISTICAL TESTS

Statistical tests are used to see whether or not the distributions of selected subduction parameters in the bins containing $M_w \geq 8.0$ earthquakes are significantly different than the global distributions of these parameters (Figure 5). Subduction parameters examined are slip vector residuals (SVR), obliquity, relative plate convergence rate (V), the arc-parallel component of plate convergence rate (Vt), the arc-

TABLE 1. List of $M_w \geq 8.0$ earthquakes

Event	Date	Latitude	Longitude	Depth, km	*Mw*	*Ms*	*Ms*1	Obl., deg	N	Slip Vector Residual	Moment 10^{19}N m	Comments
1	Jan. 31, 1906	1.00	-81.50	0	8.8	8.2	8.1	23	4	6.5 ± 5.3	210-1400	
2	Aug. 17, 1906	-33.00	-72.00	0	8.2	8.1	7.7	20	58	6.0 ± 10.3	49	
3	Aug. 17, 1906	51.00	179.00	0	-	8.2	8.0	50	14	18.4 ± 7.8	660	
4	April 15, 1907	17.00	-100.00	0	-	8.0	7.6	-19	17	-3.7 ± 13.3	83	
5	May 1, 1915	47.00	155.00	0	-	8.0	7.8	4	36	-1.1 ± 9.3	69	
6	June 26, 1917	-15.50	-173.00	0	-	8.4	8.2	-59	61	-7.5 ± 27.0	120-700	
7	Sept. 7, 1918	45.50	151.50	0	-	8.2	8.0	22	56	3.8 ± 11.5	220-1400	
8	April 30, 1919	-19.00	-172.50	0	-	8.2	8.0	15	36	11.6 ± 17.3	270-500	
9	Nov. 11, 1922	-28.50	-70.00	0	(8.)	8.3	8.1	27	12	11.8 ± 20.0	1400	
10	Feb. 3, 1923	54.00	161.00	0	8.3	8.3	8.1	-5	36	-1.2 ± 9.6	700-2000	
11*	Sept. 1, 1923	35.25	139.50	0	8.0	8.2	8.0		26	-6.1 ± 28.3	76	TJ
12	Dec. 1, 1928	-35.00	-72.00	0	-	8.0	7.8	36	31	7.4 ± 8.0	44	
13	June 3, 1932	19.50	-104.25	0	-	8.2	8.0	1	7	-4.8 ± 4.3	31-152	
14	July 18, 1934	-11.75	166.50	0	-	8.1	7.9	-8	31	-11.4 ± 15.3	65	
15	Nov. 10, 1938	55.50	-158.00	0	8.2	8.3	8.1	1	3	0.6 ± 2.9	123-500	
16*	April 30, 1939	-10.50	158.50	50	-	8.0	7.8		0		69	Collision
17	May 24, 1940	-10.50	-77.00	60	8.2	7.9	7.7	-23	1	-20.8	20	R89
18	Aug. 24, 1942	-15.00	-76.00	60	8.2	8.2	8.0	-34	10	-0.9 ± 11.4	43	
19	April 6, 1943	-30.75	-72.00	60	(8.2)	7.9	7.7	17	17	5.0 ± 13.5	250	R89
20	Dec. 7, 1944	33.75	136.00	0	8.2	8.1	7.8	45	3	-1.0 ± 2.4	150	
21	Dec. 20, 1946	32.50	134.50	0	8.5	8.1	8.0	15	1	2.5	150	
22	March 4, 1952	42.50	143.00	0	8.2	8.3	8.3	16	24	-0.9 ± 6.4	144-250	
23	Nov. 4, 1952	52.75	159.50	0	9.0	8.2	8.2	-9	47	0.1 ± 9.1	3500	
24	March 9, 1957	51.30	-175.80	0	9.1	8.1	8.1	36	64	7.4 ± 9.0	1000-4000	
25	Nov. 11, 1958	44.40	148.60	60	8.3	8.1	8.1	21	87	6.8 ± 9.0	440	
26	May 4, 1959	53.20	159.80	60	8.2	7.7	8.2	-5	45	0.3 ± 9.1	126	R89
27	May 22, 1960	-38.20	-72.60	0	9.5	8.5	8.5	22	11	9.2 ± 12.5	16000-32000	
28	Dec. 13, 1963	44.90	149.60	0	8.5	8.1	8.1	23	90	5.5 ± 9.5	500-750	
29*	March 28, 1964	61.10	-147.50	23	9.2	8.4	8.4		0		510-7500	Obl. unknown
30	Feb. 4, 1965	51.30	178.60	36	8.7	8.2	8.2	50	12	20.5 ± 7.3	111-1400	
31	Oct. 17, 1966	-10.70	-78.60	38	8.1	7.8	7.8	-23	2	-15.1	200	L82
32	May 16, 1968	40.90	143.40	9	8.2	8.1	8.1	-9	67	-1.7 ± 7.8	280	
33	Aug. 11, 1969	43.40	147.80	40	8.2	7.8	8.2	23	69	7.7 ± 7.9	220	R89
34*	July 14, 1971	-5.50	153.90	40	8.0	7.8	7.8		33	-31.6 ± 20.5	120	L82, TJ
35*	July 26 1971	-4.90	153.20	40	8.1	7.7	7.7		16	-31.0 ± 30.5	180	L82, TJ
36	Oct. 3, 1974	-12.20	-77.60	9	8.1	7.6	7.6	-30	3	-11.5 ± 20.7	90-150	L82
37	Dec. 12, 1979	1.60	-79.40	24	8.2	7.6	7.6	23	13	12.3 ± 11.7	170-290	CMT
38	March 3, 1985	-33.92	288.29	41	8.0	7.8	7.8	36	51	7.1 ± 8.8	35-115	CMT
39	Sept. 19, 1985	17.91	258.01	21	8.0	8.1	8.1	-11	21	-7.6 ± 7.7	83-160	CMT
40	May 7, 1986	51.33	184.57	31	8.0	7.7	7.7	27	67	7.8 ± 8.9	100-145	CMT

Ms from *Abe* [1984]; *Ms*1 and moment ranges from *Pacheco and Sykes* [1992]; *Mw* from *Kanamori* [1983], (L82) *Lay et al.* [1982], and (R89) *Ruff* [1989]. Events marked with an * were not used for reasons given in comments (TJ indicates event is near triple junction). Obl. = obliquity. Slip vector residuals are for events within 200 km of the epicenter of the great earthquake (data are described in the text). N is the number of slip vectors used.

normal plate convergence rate (Vn), the arc-parallel component of forearc motion (Vs), and dip angle of the subducting plate. I also test the effects of weighting the slip vectors and whether or not the inclusion of SVR from trenches behind which backarc spreading occurs or for which the pole of rotation is poorly known changes the conclusions.

First I test the null hypothesis that the distribution of SVR in forearc bins with $M_w \geq 8.0$ earthquakes is simply a random sample of all forearc bins. The 203 bins from all trenches have a mean SVR of 1.1° and standard deviation σ_{all}=20.6° while the 31 M8 bins have a mean of 1.4° and standard deviation σ_{M8}=8.8° (Figure 5a). Assuming that the means are the same, the F-test statistic ($F = \sigma^2_{all}/\sigma^2_{M8}$) at the 1% probability level for 202 and 30 degrees of freedom is 2.1 whereas the computed value is 5.5 (Table 3; trial A), indicating that the probability of the null hypothesis being true is much less than 1%. The null hypothesis also fails the F-test for different ways of weighting the bin averages and in cases where bins with fewer than 3 SVR are omitted (Table 3).

To test the significance of the difference between the means and standard deviations, I selected values at random from the average residuals in all the bins. For example, to test whether or not the SVR in the M8 bins are a random sample of global SVR bin averages, I randomly selected 31 SVR averages from the 203 global bins and calculated the trial mean and standard deviation for the 31 values. This random selection test was done 10,000 times and the percentage of trials in which the trial mean, μ_t, exceeded the actual mean of the M8 bins, μ_{M8}, and in which the trial standard deviation, σ_t, was less than σ_{M8} was recorded. In trial A (Table 3), in which all bins are weighted equally, none of the 10,000 trial values of σ_t was less than σ_{M8}, consistent with the outcome of the F-test. Hence, the hypothesis that the SVR near great earthquakes are a random sample of the global SVR distribution can be rejected with high confidence. The high value for P(μ), the percent of times the trial mean exceeded the mean of the M8 bins, shows that the means are not significantly different (Table 3).

The standard deviation for individual (i.e., not binned) SVR is 20.1° and for those near great earthquakes it is 14.5° (Figure 6a). The F-statistic for these distributions is 1.9 while the value for 1% confidence for 2040 and 470 degrees of freedom is 1.18. A test in which 471 residuals were repeatedly selected at

TABLE 2. Parameters for Bins Containing $M_w \geq 8.0$ Earthquakes

Trench	Latitude °N	Longitude °E	Plate Vector	σ	Slip Vector	σ	SVR	σ	N	Obli-quity	σ	Plate Rate	Events in bin
South America													
	-38.01	285.21	79.3	0.9	87.3	13.8	8.7	13.8	10	21.9	1.3	84	27
	-34.16	286.85	78.5	0.9	85.5	7.4	7.6	7.4	20	35.6	3.2	84	12,38
	-32.81	287.33	78.3	0.9	84.5	9.8	6.7	9.8	31	19.9	4.4	84	2
	-30.13	287.59	78.1	1.0	87.1	10.1	9.5	10.1	9	17.3	0.9	84	19
	-27.47	288.25	77.7	1.0	89.1	20.9	11.8	20.9	12	26.7	2.7	84	9
	-15.18	283.51	79.8	1.0	81.9	6.1	2.5	6.1	7	-33.7	1.6	81	18
	-13.86	282.30	80.4	1.0	73.0	---	-6.9	---	2	-30.3	1.1	80	36
	-10.88	280.28	81.4	0.9	60.0	---	-20.8	---	1	-22.7	1.3	78	17,31
	1.13	279.47	80.9	1.1	87.5	5.4	7.0	5.4	6	23.3	4.4	70	1,37
Mid America													
	16.05	260.25	35.0	1.5	34.3	18.3	1.2	18.2	10	-18.7	0.5	61	4
	16.96	257.60	36.2	1.7	25.8	8.0	-7.4	7.9	6	-11.1	2.1	54	39
	18.35	255.29	36.0	1.9	31.0	4.0	-2.6	4.0	3	1.3	1.5	48	13
Aleutians													
	54.26	204.00	333.2	1.3	331.0	6.3	-2.6	6.2	6	1.3	7.7	63	15
	50.52	185.50	320.9	1.1	330.4	9.3	9.1	9.2	47	27.1	1.3	73	40
	50.29	183.32	319.6	1.0	328.2	9.4	7.9	9.5	30	36.5	4.7	74	24
	50.33	179.02	317.4	1.0	340.2	11.0	22.3	11.2	19	49.9	2.9	76	3,30
Kuriles													
	53.34	162.72	309.3	0.9	305.0	10.5	-3.3	10.6	9	-4.7	1.1	79	10
	52.59	161.86	308.5	0.9	305.7	10.2	-1.9	10.2	19	-5.0	1.0	80	26
	51.81	161.08	307.9	0.9	309.5	9.1	2.2	9.1	16	-9.0	1.1	80	23
	46.89	155.14	303.5	0.8	300.6	10.5	-2.4	10.6	12	3.6	0.4	83	5
	44.97	152.41	301.7	0.8	309.6	11.8	8.4	11.8	27	22.2	1.3	84	7
	43.94	150.41	300.4	0.8	306.1	8.2	6.1	8.2	32	23.0	0.8	85	28
	43.37	149.41	299.8	0.8	310.1	8.5	10.6	8.5	30	20.9	0.5	85	25
	42.78	148.42	299.2	0.8	304.6	7.6	5.8	7.5	19	23.0	1.2	85	33
	40.84	144.93	297.1	0.8	294.8	6.2	-1.8	6.2	5	15.6	2.0	86	22
Japan													
	40.19	144.44	296.7	0.8	292.9	8.6	-3.1	8.6	22	-9.3	8.7	86	32
Nankai													
	32.44	136.27	307.8	4.9	308.0	---	-1.6	---	2	45.3	11.8	41	20
	31.73	134.29	309.0	4.6	306.0	---	-6.2	---	1	14.7	6.5	44	21
Solomon													
	-12.56	165.80	79.6	0.6	69.0	14.8	-10.9	14.8	23	-8.5	3.2	94	14
Tonga													
	-15.12	187.38	274.0	0.6	257.0	29.6	-16.6	29.6	22	-59.0	10.2	88	6
	-18.84	187.37	274.3	0.6	276.9	18.0	3.3	17.8	13	14.7	1.9	82	8

Latitude and longitude are at the trench at the midpoint of the bin. σ is the standard deviation for the parameter preceding it (not given if the number of slip vectors is less than 3). SVR is slip vector residual. N is the number of slip vectors in the bin. Plate rate is in mm/yr. Events in each bin are numbered as in Table 1.

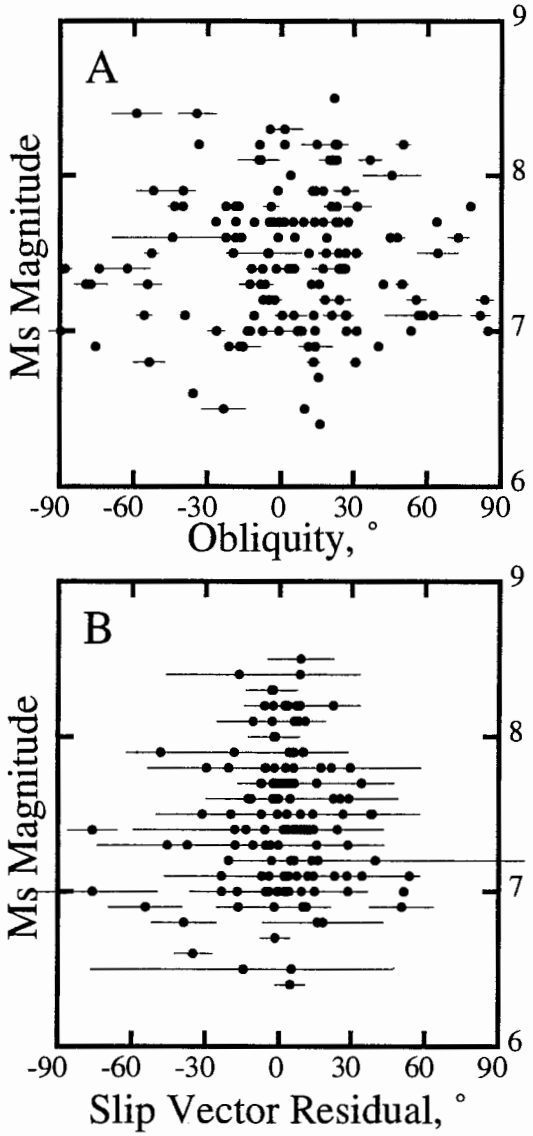

Fig. 3. (a) Relationship of the obliquity of each bin to the magnitude (M_s) of the largest earthquake occurring in that bin. Note the scatter in obliquities for all magnitudes. (b) Relationship of the average slip vector residual of each bin to the largest earthquake occurring in that bin. The scatter is greatly reduced for the larger magnitudes which seem to have smaller slip vector residuals than the lower magnitudes.

random from the 2041 residuals also indicates that the standard deviations of the two populations are significantly different (Figure 6a). The standard deviation of SVR near great earthquakes is only 2° larger the standard deviation of the misfit to trench slip vectors in the NUVEL-1 solution (*C. DeMets*, personal communication, 1992). Slip vectors near great earthquakes may be only slightly biased indicators of plate motion, insofar as the trench slip vectors used in NUVEL-1 are selected from undeforming plate boundaries.

As shown in Table 3, the choice of weighting the bin averages is not important. The weighting method for individual SVR also makes little difference in the statistical argument. For example, I weighted the slip vectors according to their estimated angular uncertainty based on the size of the earthquake (the details of and the reasoning behind this scheme are given by *DeMets* [1992]); such weighting produced the values σ_{M8}=8.6° and σ_{all}=20.5° (F=5.7). At the other extreme, giving each slip vector a weight equal to the seismic moment gave the values σ_{M8}=6.7° and σ_{all}=19.9° (F=8.7). The decrease in σ_{M8} from 8.8° to 6.7° when weighted by seismic moment (compared to equal weighting) suggests that the larger earthquakes show the plate motion better than smaller earthquakes. While this argues for weighting slip vectors by seismic moment, one still has to worry about possible pitfalls with overemphasis of a few large events [*DeMets*, 1992; *McCaffrey*, 1993]. All these weighting schemes give an F-test statistic of much greater than 2.1, indicating that the null hypothesis fails at the 1% level regardless of the weighting used.

Excluding the two arcs where the slip vector residuals are the largest (Mariana and New Hebrides) gives σ_{all}=17.3° (N=184) and σ_{M8}=8.8° (unchanged because no great earthquakes occur at these arcs), for F=3.8 which is still well above the 1% confidence level of 2.1 and gives P(σ)=0.10%. Excluding all

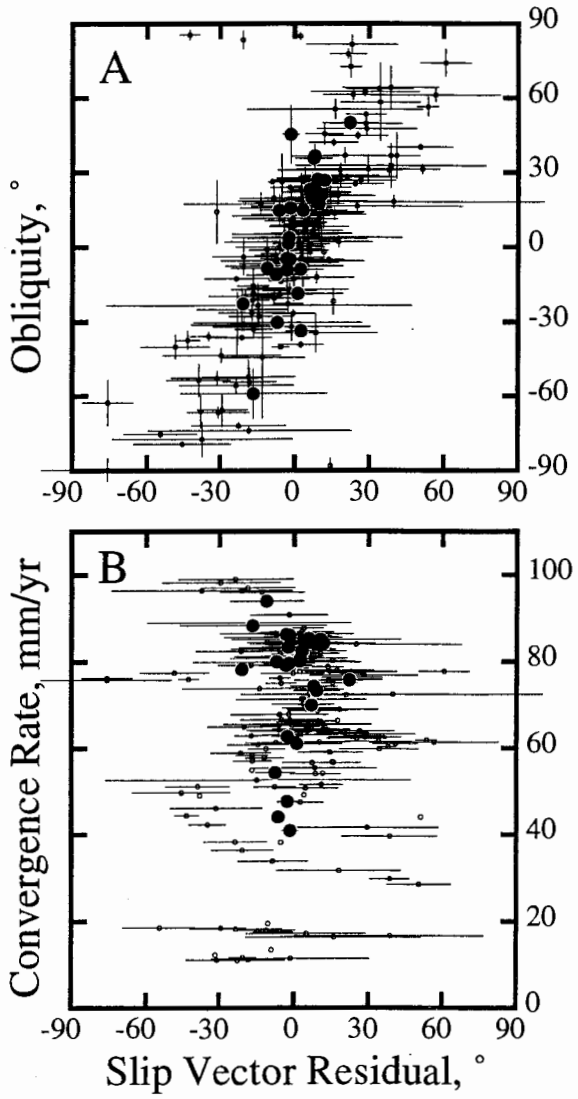

Fig. 4. (a) Relationship between the slip vector residual and obliquity for all bins. Large dots are for forearc bins containing $M_w \geq 8.0$ earthquakes (Table 2) which show a wide range of obliquities but a narrow range of residuals. (b) Relationship of the slip vector residual to convergence rate for all bins. Again the large dots are for bins containing $M_w \geq 8.0$ earthquakes.

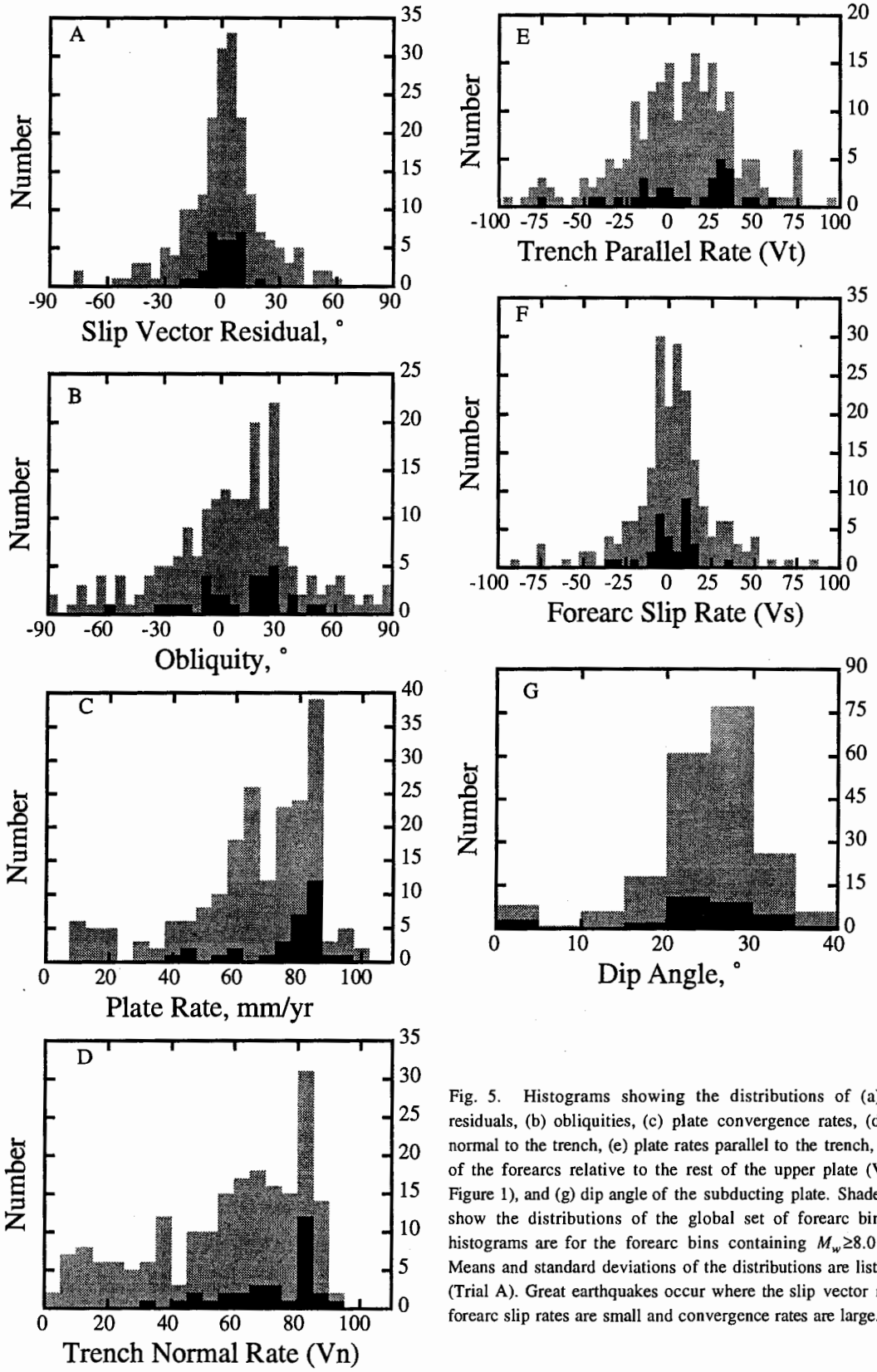

Fig. 5. Histograms showing the distributions of (a) slip vector residuals, (b) obliquities, (c) plate convergence rates, (d) plate rates normal to the trench, (e) plate rates parallel to the trench, (f) slip rates of the forearcs relative to the rest of the upper plate (V_S shown in Figure 1), and (g) dip angle of the subducting plate. Shaded histograms show the distributions of the global set of forearc bins and black histograms are for the forearc bins containing $M_w \geq 8.0$ earthquakes. Means and standard deviations of the distributions are listed in Table 3 (Trial A). Great earthquakes occur where the slip vector residuals and forearc slip rates are small and convergence rates are large.

arcs behind which active backarc spreading is known or suspected (Mariana, Izu, New Hebrides, Sandwich, and Tonga) gives σ_{all}=16.0° (N=145) and σ_{M8}=8.2° (N=29) for F=3.8 ($F_{1\%}$=2.15) and P(σ)=0.19%. Exclusion of these arcs reduces the standard deviation σ_{all} by too little, from 20.6° to 16.0°, compared to σ_{M8} which is reduced from 8.8° to 8.2°, to suggest that arcs with active back-arc spreading alone control the increase in variance between the M8 bins and the global bins. Distributions of the individual slip vector residuals lead to the same conclusion (Figure 6b).

To test whether or not SVR at trenches with great earthquakes match the global distribution, I exclude bins from

TABLE 3. Statistics of Forearc Bins With and Without $M_w \geq 8$ Earthquakes

	All Bins		*$M_w \geq 8$ Bins*		F	P(σ)	P(μ)
	μ_{all}	σ_{all}	μ_{M8}	σ_{M8}			
	Trial A $N_b \geq 1$ $W_b=1$ $N_{all}=203$ $N_{M8}=31$ $F_{1\%}=2.07$						
SVR	1.1	20.6	1.4	8.8	5.46	0.00	47.90
Obl	4.1	34.3	7.5	24.5	1.96	2.63	28.62
Vel	66.3	20.9	76.2	13.5	2.38	1.40	0.14
Vt	5.5	33.5	9.1	30.8	1.18	32.22	26.67
Vs	2.8	25.6	1.6	13.5	3.57	0.81	59.80
Vn	55.8	24.0	69.1	14.9	2.60	0.18	0.08
Dip	22.5	6.9	21.7	8.5	0.66	88.42	72.95
	Trial B $N_b \geq 3$ $W_b=1$ $N_{all}=161$ $N_{M8}=27$ $F_{1\%}=2.22$						
SVR	1.3	18.6	2.9	8.0	5.48	0.01	35.48
Obl	4.3	31.7	8.3	23.4	1.84	4.99	26.33
Vel	68.0	20.6	78.5	10.8	3.61	0.52	0.08
Vt	6.0	31.8	11.6	30.3	1.10	42.48	19.43
Vs	2.5	21.9	3.4	12.9	2.88	2.12	42.07
Vn	59.0	22.9	71.4	12.7	3.29	0.12	0.07
Dip	23.6	4.9	24.0	4.7	1.06	55.84	35.72
	Trial C $N_b \geq 1$ $W_b=N_b$ $N_{all}=203$ $N_{M8}=31$ $F_{1\%}=2.07$						
SVR	3.0	16.2	4.0	8.3	3.78	0.02	26.18
Vs	3.7	20.2	5.0	13.7	2.15	1.82	33.31
Dip	23.8	4.3	24.0	4.6	0.90	8.65	13.55
	Trial D $N_b \geq 3$ $W_b=N_b$ $N_{all}=161$ $N_{M8}=27$ $F_{1\%}=2.22$						
SVR	3.0	15.6	4.1	8.3	3.57	0.06	25.09
Vs	3.7	19.5	5.1	13.7	2.02	4.85	30.32
Dip	24.0	3.9	24.2	4.0	0.95	25.94	29.33
	Trial E $N_b \geq 1$ $W_b=\sigma_b^{-2}$ $N_{all}=203$ $N_{M8}=31$ $F_{1\%}=2.07$						
SVR	1.8	18.8	2.3	6.2	9.15	0.00	41.93
Obl	5.4	22.3	5.0	16.8	1.75	51.74	52.53
Vel	66.6	21.3	77.3	12.2	3.04	0.64	0.10
Vt	-11.6	42.4	4.8	23.5	3.25	88.74	53.85
Vs	1.6	12.1	-4.7	6.9	3.04	0.29	81.00
Vn	56.8	23.9	70.5	13.3	3.23	0.04	0.02
Dip	26.9	5.9	23.5	5.0	1.39	20.06	30.04
	Trial F $N_b \geq 3$ $W_b=\sigma_b^{-2}$ $N_{all}=161$ $N_{M8}=27$ $F_{1\%}=2.22$						
SVR	1.8	18.6	2.4	6.2	8.97	0.01	44.27
Obl	-3.3	20.7	5.7	16.5	1.58	58.59	52.36
Vel	68.0	20.6	78.5	10.8	3.61	0.59	0.10
Vt	-2.7	28.4	5.6	23.3	1.49	90.10	56.17
Vs	1.9	12.1	-4.0	5.5	4.82	0.14	81.93
Vn	59.0	22.9	71.4	12.7	3.29	0.16	0.12
Dip	26.9	5.9	23.5	4.9	1.42	67.31	55.27
	Trial G New Poles $N_b \geq 1$ $W_b=1$ $N_{all}=205$ $N_{M8}=31$ $F_{1\%}=2.07$						
SVR	2.1	18.9	0.4	9.4	4.03	0.56	69.08
Obl	4.7	32.0	6.6	23.9	1.79	6.28	36.34

μ, mean; σ, standard deviation. The subscript t indicates values from random sampling trials. SVR, slip vector residual; Obl, obliquity; Vel, convergence rate; Vn, trench-normal rate; Vt, trench-parallel rate; Vs, forearc arc-parallel rate; Dip, dip angle of the subducting plate taken from dips of earthquake fault planes. Angles are in degrees and rates in mm/yr. For each trial a minimum number N_b of slip vectors in the bin was used, weighting W_b of each bin was either uniform, based on the number of slip vectors in the bin (Obl, Vel, Vt, and Vn do not depend on the slip vectors so are not included in trials C and D), or was inversely proportional to the variance of the particular parameter in the bin (σ=100 for bins with 1 or 2 slip vectors). Total number of bins is N_{all} and the number with $M_w \geq 8$ earthquakes is N_{M8}. $F=(\sigma_{all}/\sigma_{M8})^2$. F values of greater than $F_{1\%}$ indicate that at the 1% confidence level the $M_w \geq 8.0$ distributions are not a random sample of all the bins. P(σ) is the percent of 10,000 trials in which the standard deviation of randomly selected values was less than or equal to the standard deviation of the values for bins containing $M_w \geq 8.0$ earthquakes. P(μ) is the percent of such trials in which the mean of the randomly selected values was greater than or equal to the mean of the values for bins containing $M_w \geq 8.0$ earthquakes. Trial G was based on new poles of rotations for trenches as discussed in the text.

all trenches that have not had $M_w \geq 8$ earthquakes (i.e., Mariana, Izu, New Hebrides, Sandwich, Java, Southern Ryukyu, Antilles, and the Chile trench south of 46°S), resulting in a standard deviation of all bins σ_{all}=13.7° (N=135) which is still significantly greater than σ_{M8}=8.8° at the 1% confidence level (F=2.4; $F_{1\%}$=2.1). The standard deviation of the global individual SVR is reduced to 16.3° which is slightly greater than that of 14.5° for SVR near great earthquakes (F=1.3; $F_{1\%} \approx 1.2$) and random testing gives a match 4% of the time (Figure 6c). This statistical test, that great earthquakes occur only along the low SVR sections of trenches that elsewhere can have high SVR values, gives an ambiguous result at a high level of confidence.

The hypothesis that great earthquakes occur randomly in the global set of bin obliquities cannot be rejected at a high level of confidence (Figure 5b). The standard deviation of obliquity for all bins is σ_{all} = 34.3° while σ_{M8} for obliquity is 24.5° (Figure 5b and Table 3, trial A). The F-test statistic is 1.96 which is less than the value of 2.1 for a 1% probability. In a random sampling test, 31 samples of obliquity from the 203 bins gave a standard deviation of 24.5° or less, 2.6% of the times. This percentage is high enough that we cannot reject the null hypothesis that, for obliquity, the $M_w \geq 8$ earthquakes occur in bins that are a random sample of the global bins (although it cannot be proven that they are a random sampling of all the bins). Thus, great earthquakes do not occur preferentially where subduction is perpendicular to the trench.

Table 3 shows similar tests for the significance of convergence rate (Vel), arc-parallel plate rate (Vt), arc-normal plate rate (Vn), arc-parallel forearc motion rates (Vs), and dip angle being different in the M8 bins than in the global distribution. Also shown are results of different bin weighting schemes and removing bins with fewer than 3 SVR. Significant features are that the plate rate (Vel) and arc-normal rate (Vn) for M8 bins have higher means than the global distribution and that Vn has a smaller standard deviation. Therefore, great earthquakes appear to prefer large convergence rates (Figure 5c) and rates perpendicular to the trench (Figure 5d). The forearc deformation rate Vs, estimated from the SVR and convergence rates (Figure 1), also appears to be low in bins containing great earthquakes (Figure 5f and Table 3). There is no difference in trench-parallel relative rates (Vt; Figure 5e) or dip angles (Figure 5g) between bins with and without great earthquakes.

Finally, Trial G (Table 3) and Figure 6d show the SVR statistics when new poles of rotation are calculated and used for the Southern Middle America, Ryukyu, Java, New Hebrides, Mariana, and Izu trenches [*McCaffrey*, 1993]. A pole of rotation was found for each trench that minimized the sum of the squares of the slip vector residuals (see *DeMets et al.* [1990] for the fitting function and method). Slip vectors do not

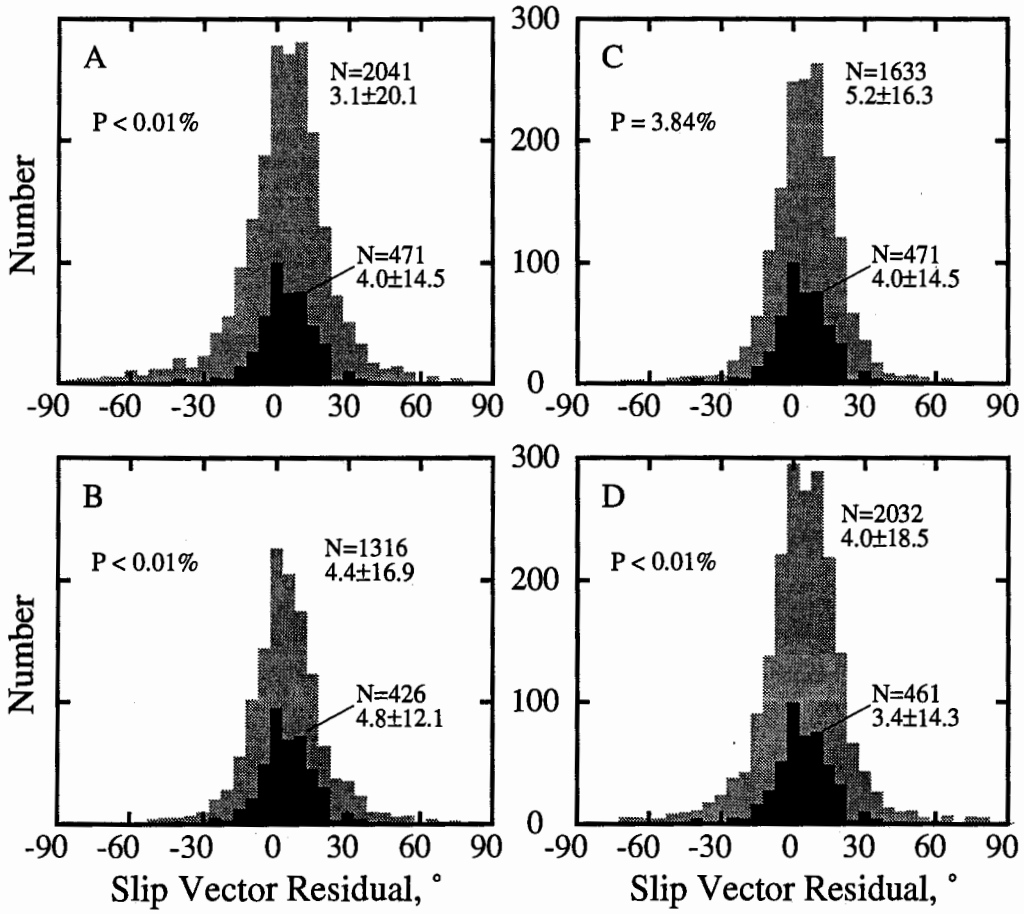

Fig. 6. Histograms of individual slip vector residuals (SVR). Shaded histograms are for all SVR and the black ones are for SVR near great earthquakes. N is the number of residuals and the mean and standard deviations are shown. P is the percent of times out of 10,000 trials that a random sample of N values taken from all SVR values had a standard deviation that was less than or equal to that of the SVR near the $M_w \geq 8$ earthquakes. A low value for P suggests that the SVR near great earthquakes is not a random sample of the global distribution. (a) SVR distributions for all trenches, (b) all trenches without active backarc spreading (Mariana, Izu, Sandwich, Tonga, and New Hebrides excluded), (c) all trenches with $M_w \geq 8$ earthquakes (Mariana, Sandwich, New Hebrides, Java, Southern Ryukyu, Izu, Antilles, and the Chile trench south of 46°S excluded), and (d) SVR distributions when new poles of rotation are calculated for the Southern Middle America (34°N, 159°W), Ryukyu (49°N, 173°W), Java (11°S, 122°E), New Hebrides (50°S, 149°W), and Mariana-Izu (10°S, 143°E) trenches. This trial minimizes the SVR for trenches at which the convergence directions are poorly constrained.

constrain plate rates so Trial G does not include rate statistics. Using these calculated poles of rotation minimizes the bias introduced into the SVR by ignorance of the actual pole of rotation and should remove any systematic rotation of the slip vectors caused by backarc spreading. Thus, the new poles of rotation minimize the inferred forearc deformation at these trenches. Nevertheless, we see the same results in the distributions of SVR and obliquities. Hence, errors in the poles of rotation for the trenches mentioned above are not causing the difference in SVR for bins with and without great earthquakes.

That great earthquakes tend to nucleate in regions where the slip vectors of thrust earthquakes are close to the expected plate convergence vector suggests that they are associated with forearcs that compensate the arc-parallel shearing force associated with oblique subduction elastically. Anelastic behavior in the down dip shear strain will not significantly deflect the slip vectors of subduction earthquakes and hence cannot be revealed with them. Nevertheless, I infer that forearcs that respond elastically to arc-parallel shear also accommodate the down-dip shearing on the thrust plane elastically; it is the down-dip shear strains that store most of the elastic energy released in great subduction earthquakes.

DISCUSSION

The global distribution of great subduction zone earthquakes has been used to reveal variability in what is called "seismic coupling" which means the force acting across the thrust interface [*Ruff and Kanamori*, 1980; *Lay et al.*, 1982]. Others interpret the distribution of great earthquakes to be influenced by variations in the areas of the faults [*Kelleher et al.*, 1974], which will affect the coupling, in the ability of large, highly stressed "asperities" to connect during rupture [*Lay et al.*, 1982], in the homogeneity of stress on the fault surface [*Lay and Kanamori*, 1981], or in the surface area of the fault that is in the unstable or conditionally stable frictional stability field [*Scholz*, 1990].

Ruff and Kanamori [1980] examined the relationship between the largest known earthquakes to occur at a particular trench and other factors that influence stress at the plate interface. Their underlying premise was that great earthquakes are a result of high seismic coupling on the thrust fault. They concluded that the magnitudes of the largest earthquakes at trenches correlate best with a linear combination of convergence rate and age of the subducting lithosphere. They explained that fast convergence of young, buoyant lithosphere increases the coupling force between the subducting slab and the forearc. *Peterson and Seno* [1984] looked at the variation in the seismic moment release rate at the trenches using the *Abe* [1981] catalog and reached the same conclusion. These and similar studies have led to the characterization of subduction zones in terms of their level of seismic coupling but still are largely based on the assumption that great thrust earthquakes indicate strong coupling between the plates. I argue here that the distinction between strongly and weakly coupled subduction zones, that is, the level of stress, cannot be based on the occurrence of great earthquakes.

For a high level of shear stress to act across a fault the material on both sides of the fault must be able to sustain the stress. Therefore, it is important to consider the rheology of the forearc in trying to understand what limits the stress on the fault. The idea that great earthquakes occur where the interplate coupling is largest assumes that the rheologies of all forearcs are the same. One can imagine that this is not true. For example, consider a forearc that is elastic and one that is effectively viscous (at a macroscopic scale). The viscous-like forearc could have higher stress than the elastic one, but the elastic one will produce larger earthquakes simply because seismic waves are the release of stored elastic strain energy. I suggest that the rapid, permanent deformation evident in some forearcs [*McCaffrey*, 1993] inhibits great earthquakes because they do not store elastic strain energy as well as elastic forearcs do. By this reasoning, the occurrence of great earthquakes tells us little about stress.

Earthquake slip vectors at oblique convergent margins can be used to estimate the ratio of the maximum horizontal shear force (F_s) per unit length of the forearc that can act on an arc-parallel vertical plane in the upper plate to the total shear force (F_t) per unit length that acts on the thrust fault by the relationship

$$\sin(\gamma - \Delta\beta) = F_s / F_t \quad (1)$$

where γ is the angle of obliquity, $\Delta\beta$ is the slip vector residual, and $\Delta\beta \leq \gamma$ (Figure 1) [*McCaffrey*, 1992]. Where $\Delta\beta$ is large, $F_s << F_t$ (the forearc is weak relative to the thrust fault in the sense that it deforms permanently at low stress) and where $\Delta\beta$ is near zero the forearc is stronger in that the shear stress on it is maintained without permanent deformation (i.e., elastically). The observation that great earthquakes occur where the slip vector residuals are small suggests that in their epicentral regions, the forearc is stiff enough to withstand the horizontal shear force associated with oblique convergence without undergoing permanent, time-dependent strain. Such forearcs probably balance the arc-parallel shear forces of oblique convergence by elastic strains, which are too small to deflect the slip vectors. It follows that these forearcs can store the elastic strains necessary to produce a great earthquake. However, because the slip vectors are sensitive only to the ratio of the forces (1), we cannot compare one forearc or thrust fault to another without making assumptions about them.

Consider first the prevailing assumption that great earthquakes imply that the force on the thrust fault, F_t, is greater than some global average [*Ruff and Kanamori*, 1980; *Lay et al.*, 1982]. If all forearcs are the same in that F_s is everywhere limited to be below a certain value and if great earthquakes occur at trenches where stress on the thrust fault is high (i.e., F_t is large), then the ratio F_s/F_t will be smallest at these trenches and $\Delta\beta \approx \gamma$ (equation 1). Hence, in this case great earthquakes should be associated with large slip vector residuals and there should be a positive correlation between great earthquakes and forearc deformation. *Jarrard* [1986] suggested such a correlation based on geologic evidence for forearc deformation. However, slip rates on forearc faults are very poorly constrained to unknown. In contrast, slip vector deflections show a negative correlation between forearc deformation and great earthquakes. I conclude that stress on the thrust fault alone cannot control the distribution of great earthquakes and that all forearcs cannot be the same.

Suppose now that all thrust faults are similar (i.e., that great earthquakes do not require force on the thrust fault that is larger than the global average). Great earthquakes occur where $\Delta\beta$ is smaller than average suggesting that they occur where F_s, the maximum shear force in the upper plate, is larger than average (equation 1; if $\Delta\beta=0$ then the ratio F_s/F_t is a maximum). Moreover, because great earthquakes do not occur where $\Delta\beta$ is large, they do not occur where F_s is smaller than average (F_s is a minimum when $\Delta\beta=\gamma$). From this I conclude that the occurrence of great earthquakes could be largely limited by the rheology of the forearc and specifically by its ability to sustain subduction forces elastically (and to store elastic strain energy). Moreover, shear forces on the thrust faults that produce great earthquakes are not necessarily higher than on faults that do not have them, although this may be true if the rheology of forearcs varies more from trench to trench than do the forces on subduction thrust faults. Inferences based on slip vector deflections suggest that forearcs do exhibit a wide range of rheologies under oblique convergence [*McCaffrey*, 1993].

The correlation of fast convergence rates with great earthquakes is explained by the notion that faster convergence will increase the normal stress across the plate interface [e.g., *Ruff and Kanamori*, 1980; *Scholz*, 1990]. Slip vector residuals are also generally smaller where the trench-normal convergence rate is large (Figure 7). In the framework of the hypothesis that forearc rheology controls the distribution of great earthquakes, I suggest that the convergence rate normal to the trench controls temperature of the forearc which in turn affects its rheology. Here I show that if the shear stress on the plate interface is less than a few tens of MPa, for a subducting plate older than 30 Ma or so [*van den Beukel and Wortel*, 1988; *Hyndman and Wang*, 1993], then the forearc will be cooled by subduction and, at large convergence rates, the average steady-state temperature of the forearc will decrease with increasing convergence rate.

Considering only heat flux from below the fault and shear heating on the fault, *Molnar and England* [1990] show that the steady-state temperature distribution T(x,z) within the hanging wall of a thrust can be approximated by

$$T(x,z) = (Q_o + \tau V)\, z / K S \quad (2)$$

where $S = 1 + b \sin\delta\, (V x / \kappa \cos\delta)^{1/2}$, x is zero at the fault and positive toward the forearc, z is positive down, Q_o is the heat flux from below, τ is the shear stress on the thrust fault, V is

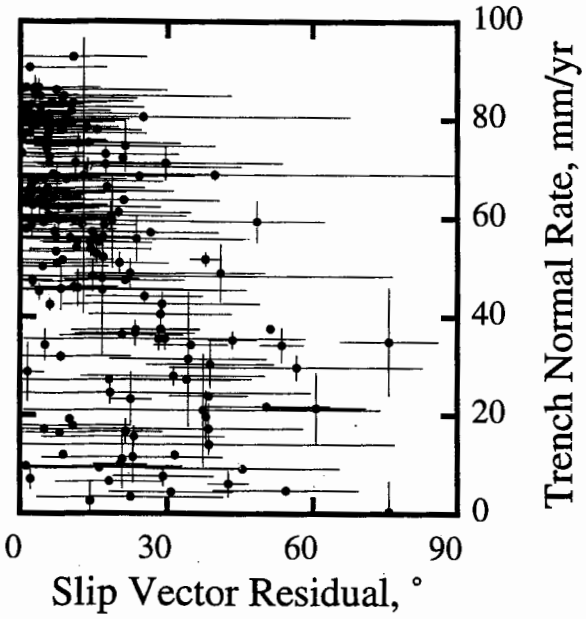

Fig. 7. Plot of the trench-normal component of plate convergence versus the slip vector residual for all bins. The residuals are much less for faster subduction perpendicular to the trench.

the trench-normal subduction rate, K is thermal conductivity, δ is the dip angle of the fault, and κ is thermal diffusivity. The factor b depends on the Peclet number (V a / κ, where a is the thickness of the lithosphere), δ, and the type of heating [*Molnar and England*, 1990]. For the parameters I use, b ranges from 0.83 to 0.96 and is nearly equal for cases of heating from below and shear heating for all values of the Peclet number [*Molnar and England*, 1990, Table 3]. In this expression the trench-normal convergence rate V appears both in a shear heating term τV and in a cooling factor S arising from advection of a cold subducting plate beneath the hanging wall. The effect on steady-state temperature in the hanging wall when shear stress on the fault is neglected is that the upper plate cools rapidly with increasing convergence rate (Figure 8).

To estimate the summed result of shear heating and advective cooling on the forearc, I calculate average temperatures in a forearc using equation (2) and parameters given in the caption to Figure 8. At convergence rates of greater than 20 mm/yr, the average temperature in the forearc wedge decreases with increasing convergence rate for a shear stress of about 20 MPa or less (Figure 9). This shear stress depends very weakly on the dip angle and diffusivity, not at all on the conductivity, but strongly on the basal heat flux Q_o. Using ranges of $10^{-6} \le \kappa \le 4.0 \times 10^{-6} m m^2/s$, $10° \le \delta \le 50°$, and $20 \le Q_o \le 100$ mW/m^2, the magnitude of shear stress on the thrust fault below which the forearc continues to cool with increasing convergence rate (i.e., the slope $dT_{av}/dV < 0$ at V=60 mm/yr) ranges from 6 to 42 MPa. For shear stress above 40 MPa the forearc will become warmer with increasing convergence rate. Again we see that high shear stress on the thrust fault favors deformation of the forearc as the increase in temperature due to shear heating should weaken it. In summary, if the decrease in the slip vector residuals with increasing arc-normal subduction rate is due to strengthening the forearc by advective cooling then the shear stress on the thrust faults must be below 40 MPa.

Heat flow measurements in forearcs are too few at present to reveal a correlation between heat flow and convergence rate, if it exists. Estimates of shear stress magnitudes on subduction thrust faults have been constrained by heat flow measurements for only a few forearcs. *Molnar and England* [1990] and *Kao and Chen* [1991] estimated shear stress magnitudes of greater than 50 MPa for the Japan, (36° to 37°N), Peru (2°S to 23°S), and Ryukyu (23°N to 31°N) subduction thrusts. *Van den Beukel and Wortel* [1988], however, obtained a significantly smaller shear stress for Japan (10 to 40 MPa), which can be explained by their inclusion of radioactive heat generation in the top 25 km of the upper plate that *Molnar and England* [1990] did not include.

Following *Molnar and England* [1990], assume that heat production rate A in the crust decays exponentially with depth,

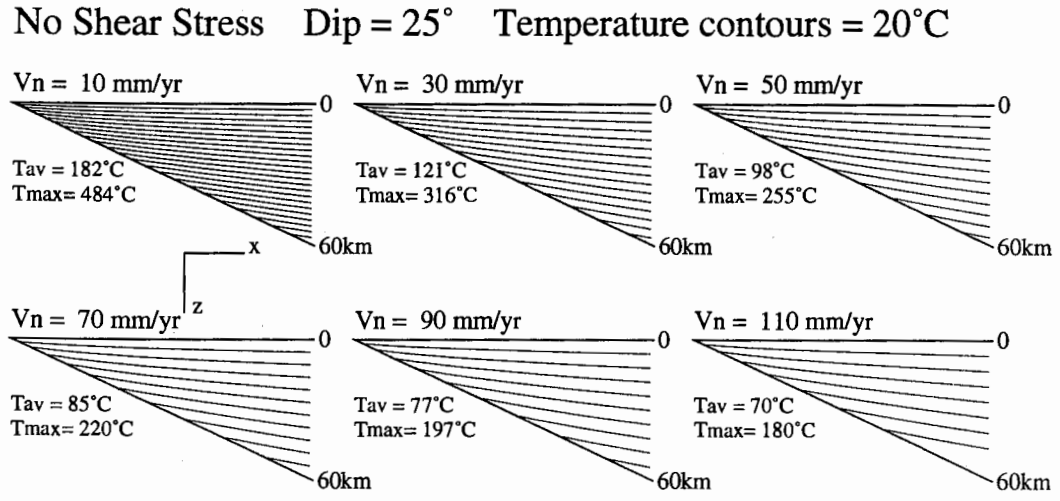

Fig. 8. Steady state isotherms within the forearc upper plate wedge above a subducting plate for different rates of subduction (V_n) and no shear stress on the thrust fault, calculated with equation (2). Tav is the average temperature in the forearc wedge and Tmax is the temperature on the fault at 60 km depth. Isotherms are every 20°C starting with 0°C at the surface. Assumed values for parameters used in this plot are: Q_o=60 mW/m^2, K=2 W/m°K, κ=10^{-6}m^2/s, and δ=25°. No vertical exaggeration.

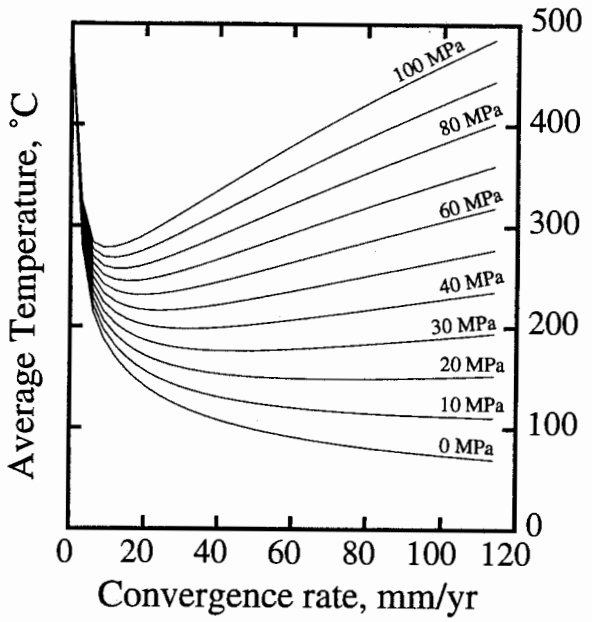

Fig. 9. Plot of the average temperature in the forearc wedge shown in Figure 8 versus the subduction rate for different values of the shear stress on the thrust fault (as labeled). Note that for low stress values the average temperature decreases with increasing rate (when rate is larger than 20 mm/yr) so that faster subduction should cool and strengthen the forearc.

$$A(z) = A_o \exp(-z/D) \quad (3)$$

where A_o is the heat generation rate at the surface and D is the depth scale for the decrease with depth (D is on the order of 10 km). The contribution, Q_R, to the surface heat flow from radioactive heat generation can be estimated by taking the depth derivative of the first two terms of equation (24) of *Molnar and England* [1990], multiplying by -K, and setting z=0,

$$Q_R = -K\, dT/dz_{(z=0)} = A_o D\ (1 - e^{-z'/D}) \quad (4)$$

where z' is the depth of the fault below the point where surface heat flow is measured. If the fault is deeper than a few tens of kilometers below the surface (D << z') (4) reduces to

$$Q_R = A_o D. \quad (5)$$

Van den Beukel and Wortel [1988] used a uniform heat production rate of 0.4 to 0.9 $\mu W/m^3$ throughout a 25 km thick forearc. If all of this heat left through the surface, the increase in heat flow would be $h_c A_c$ where h_c is the thickness of the radiogenic layer and A_c is the production rate. Hence, the contribution in their models could be from 10 to as much as 22 mW/m^2, which is more than half of the observed amount. If the total radioactive production rate used by *Van den Beukel and Wortel* [1988] is put into the form of (3), for values of D between 7 and 14 km, A_o varies from 2.6 to 1.5 $\mu W/m^3$ and the product (5) for this range gives 18 to 21 mW/m^2 of radiogenically produced surface heat flow. Again radiogenic heat production in the forearc appears to produce roughly half of the heat flow in the model of *Van den Beukel and Wortel* [1988].

If half of the surface heat flow in the *Van den Beukel and Wortel* [1988] model comes from radiogenic heat production then their shear stress estimate will be significantly lower than that of *Molnar and England* [1990] who neglected it. If all of the surface heat flow comes from below the fault and shear heating on the thrust fault then the shear stress can be estimated by

$$\tau = (SQ - Q_o)/V$$

where Q is the observed surface heat flow and Q_o is the flux from below the fault [*Molnar and England*, 1990]. If Q is overestimated by a factor of 2 by including in it heat flow due to radioactivity in the forearc wedge, τ will be high by a factor of 2.5 (for values of other parameters used by *Molnar and England* [1990, Table 4] for the Japan trench; i.e., Q=34 mW/m^2, S=9.5, Q_o=50 mW/m^2). If one-third of the heat flow is from radiogenic sources, the shear stress estimate will be 60% too high. Hence, if radioactive heat production is important in the Japan forearc, as *Van den Beukel and Wortel* [1988] suggest, then the shear stress on the thrust fault could be considerably lower than the estimates of *Molnar and England* [1990]. A similar argument could be made for the estimates of *Kao and Chen* [1991] for the Ryukyu arc. In view of the uncertainty in rates of radiogenic heat production in forearcs, we cannot rule out low shear stress on subduction thrust faults on the basis of surface heat flow measurements.

Another factor that must be important in the global distribution of great earthquakes is the frictional slip stability conditions on the thrust interface [*Dietrich*, 1981; *Ruina* 1983; *Tse and Rice*, 1986]. Unstable stick-slip (i.e., earthquakes) occurs when the kinetic friction is less than the static friction, a property of the system called velocity weakening. *Scholz* [1990] suggests that great earthquakes occur on thrust faults that have a high portion of their area in the unstable and conditionally stable frictional stability fields. Instability of a fault is increased by a smoother fault surface, less gouge, greater normal stress, lower temperature, and a less stiff loading system [*Scholz*, 1990]. Of these factors that can be addressed by this study, I infer that lower temperatures and smoother fault surfaces correlate positively with great earthquakes while greater normal stresses and less stiff systems do not.

The argument for lower temperatures on the thrust faults that contain great earthquakes is based on the calculation above that faster subduction cools the thrust interface and the forearc, when shear stress is low, and the correlation of great earthquakes with high trench-normal convergence rates. More rigorous calculations of the thermal controls on the downdip length of the fault in the unstable field are presented by *Hyndman and Wang* [1993] and *Tichelaar and Ruff* [1993]. *Hyndman and Wang* [1993], in particular, show that faster convergence or subduction of older oceanic lithosphere significantly increases the area of the fault that is thermally within the unstable field.

Deformation of the forearc above the subduction thrust fault may also inhibit stick-slip instability by decreasing the smoothness of the thrust fault (*P. Molnar*, personal communication, 1993). Even if the faults within the forearc that intersect the main thrust fault do not significantly change the stability, they may act to inhibit great earthquakes by increasing the heterogeneity of stress on the thrust fault. Stress heterogeneity, or the presence of stress barriers [*Lay and*

Kanamori, 1981], inhibits the expansion of earthquake rupture to large areas and results in frequent small earthquakes rather than great ones.

The inference that forearcs that produce great earthquakes are more elastic (i.e., stiffer) than those that do not seems to contradict the observation that increased stiffness of a system inhibits stick-slip behavior [*Scholz*, 1990]. *Tse and Rice* [1986] suggest that instability will occur on a crustal fault where the temperature is below about 300°C, probably due to some fundamental change in the frictional response at the contact surface. If the thermal mechanism for stiffening the forearc that I have proposed above is correct then the fault zone is also cooled in the process. Hence, cooling of the forearc and cooling of the fault zone have competing effects on the stability of the fault. The simple thermal calculations (Figure 8) indicate that the rate of change of temperature with convergence rate is similar for the fault and the forearc. The net effect of cooling both will be to increase the instability of the fault if fault stability is more sensitive to a decrease in temperature at the fault than it is to an increase in stiffness of the surrounding material due to a similar change in temperature.

CONCLUSIONS

The rheology of forearcs is important to consider in our attempt to understand the mechanism by which great earthquakes are generated. It makes intuitive sense that great earthquakes occur where the stresses on the plate boundary are high, and this has been our prevailing notion for some time. However, this assumes that all forearcs are rheologically the same. If they are the same then we would expect more evidence of forearc deformation in regions of expected higher stress, that is, where the great earthquakes occur, than in regions of low stress. Inferences of forearc deformation based on observations of subduction zone earthquake slip vector deflections in regions of oblique convergence suggest that the opposite is true, that the forearcs in the epicentral regions of past great earthquakes are characterized by little permanent time-dependent anelastic deformation. This paradox can be explained by revising our assumptions about the stress on the subduction zone thrust faults that produce great earthquakes and the similarity of forearcs. I suggest that global variability in forearc rheology, possibly thermally controlled, provides a more plausible explanation for the distribution of great earthquakes than do different levels of stress on different subduction zone thrust faults.

Acknowledgments. Thanks to Renata Dmowska, Chris Scholz, Teng-fong Wong, and Peter Molnar for helpful reviews or discussions or both, to Chuck DeMets and Don Argus for supplying slip vectors, to Dallas Abbott for heat flow data, and to Karen Boswell and Mike Gaffey for discussions of statistics. Supported by NSF grants EAR-8903762 and EAR-8908759.

REFERENCES

Abe, K., Magnitudes of large shallow earthquakes from 1904 to 1980, *Phys. Earth Planet. Inter.*, *27*, 72-92, 1981.

Cloos, M., Thrust-type subduction-zone earthquakes and seamount asperities: A physical model for seismic rupture, *Geology*, *20*, 601-604, 1992.

DeMets, C., Oblique convergence and deformation along the Kuril and Japan trenches, *J. Geophys. Res.*, *97*, 17615-17625, 1992.

DeMets, C., Earthquake slip vectors and estimates of present-day plate motions, *J. Geophys. Res.*, *98*, 6703-6714, 1993.

DeMets, C., R.G. Gordon, D.F. Argus and S. Stein, Current plate motions, *Geophys. J. Int.*, *101*, 425-478, 1990.

Dietrich, J.H., Constitutive properties of faults with simulated gouge, in *Mechanical Behavior of Crystal Rocks, Geophys. Monogr. Ser.*, vol. *24*, edited by N.L. Carter, M. Friedman, J.M. Logan, and D.W. Stearns, 103-120, AGU, Washington D.C., 1981.

Dziewonski, A.M., T.-A. Chou, and J.H. Woodhouse, Determination of earthquake source parameters from waveform data for studies of global and regional seismicity, *J. Geophys. Res.*, *86*, 2825-2852, 1981.

Hyndman, R.D., and K. Wang, Thermal constraints on the zone of major thrust earthquake failure: The Cascadia subduction zone, *J. Geophys. Res.*, *98*, 2039-2060, 1993.

Jarrard, R.D., Relations among subduction parameters, *Rev. Geophys.*, *24*, 217-284, 1986.

Kanamori, H., Global seismicity, *Earthquakes: Observation, Theory and Interpretation*, edited by H. Kanamori and E. Boschi, p. 597-608, North-Holland, 1983.

Kanamori, H.., Rupture process of subduction-zone earthquakes, *Annu. Rev. Earth Planet. Sci.*, *14*, 293-322, 1986.

Kao, H., and W.-P. Chen, Earthquakes along the Ryukyu-Kyushu arc: Strain segmentation, lateral compression, and the thermomechanical state of the plate interface, *J. Geophys. Res.*, *96*, 21,443-21,485, 1991.

Kelleher, J., and W. McCann, Buoyant zones, great earthquakes, and unstable boundaries of subduction, *J. Geophys. Res.*, *81*, 4885-4896, 1976.

Kelleher, J., J. Savino, H. Roulette, and W. McCann, Why and where great thrust earthquakes occur along island arcs, *J. Geophys. Res.*, *79*, 4889-4899, 1974.

Lay, T., and H. Kanamori, An asperity model of large earthquake sequences, in *Earthquake Prediction: An International Review*, *Maurice Ewing Ser.* vol. *4*, edited by D.W. Simpson and P.G. Richards, pp. 579-592, AGU, Washington, D.C., 1981.

Lay, T., H. Kanamori, and L. Ruff, The asperity model and the nature of large subduction zone earthquakes, *Earthquake Predict. Res.*, *1*, 3-71, 1982.

McCaffrey, R., Slip vectors and stretching of the Sumatran forearc, *Geology*, *19*, 881-884, 1991.

McCaffrey, R., Oblique plate convergence, slip vectors, and forearc deformation, *J. Geophys. Res.*, *97*, 8905-8915, 1992.

McCaffrey, R., Global variability in subduction thrust zone - forearc systems, *Pure Appl. Geophys.*, in press, 1993.

Molnar, P., and P. England, Temperature, heat flux, and frictional stress near major faults, *J. Geophys. Res.*, *95*, 4833-4856, 1990.

Pacheco, J.F., and L.R. Sykes, Seismic moment catalog of large shallow earthquakes, 1900 to 1989, *Bull. Seismol. Soc. Amer.*, *82*, 1306-1349, 1992.

Pacheco, J.F., L.R. Sykes, and C.H. Scholz, Nature of seismic coupling along simple plate boundaries of the subduction type, *J. Geophys. Res.*, in press, 1993.

Perez, O.J., and K.H. Jacob, Tectonic model and seismic potential of the eastern Gulf of Alaska and Yakataga seismic gap, *J. Geophys. Res.*, *85*, 7132-7150, 1980.

Peterson, E.T., and T. Seno, Factors affecting seismic moment release rates in subduction zones, *J. Geophys. Res.*, *89*, 10,233-10,248, 1984.

Ranken, B., R.K. Cardwell, and D.E. Karig, Kinematics of the Philippine Sea plate, *Tectonics*, *3*, 555-575, 1984.

Ruff, L., Do trench sediments affect great earthquake occurrence in subduction zones?, *Pure Appl. Geophys.*, *129*, 263-282, 1989.

Ruff, L., and H. Kanamori, Seismicity and the subduction process, *Phys. Earth Planet. Inter.*, *23*, 240-252, 1980.

Ruina, A.L., Slip instability and state variable friction laws, *J. Geophys. Res.*, *88*, 10359-10370, 1983.

Scholz, C.H., *The Mechanics of Earthquakes and Faulting*, 439 pp., Cambridge University Press, New York, 1990.

Seno, T., T. Moriyama, S. Stein, D.F. Woods, C. Demets, D. Argus, and R. Gordon, Redetermination of the Philippine Sea plate motion, *Eos Trans. AGU*, *68*, 1474, 1987.

Tichelaar, B.W., and L.J. Ruff, Depth of seismic coupling along subduction zones, *J. Geophys. Res.*, *98*, 2017-2037, 1993.

Tse, S.T., and J.R. Rice, Crustal earthquake instability in relation to the depth variation of frictional slip properties, *J. Geophys. Res.*, *91*, 9452-9472, 1986.

Uyeda, S., and H. Kanamori, Back-arc opening and the mode of subduction, *J. Geophys. Res.*, *84*, 1049-1061, 1979.

Van den Beukel, J., and R. Wortel, Thermo-mechanical modeling of arc-trench regions, *Tectonophysics*, *154*, 177-193, 1988.

R. McCaffrey, Department of Earth and Environmental Sciences, Rensselaer Polytechnic Institute, Troy, NY 12180-3590.

(Received June 4, 1992;
revised February 8, 1993;
accepted February 18, 1993.)